DS2MA: A Deep Learning-Based Spectrum Sensing Scheme for a Multi-Antenna Receiver

Keunhong Chae and Yusung Kim, *Member, IEEE*

***Abstract*—In this letter, we propose a novel deep learning-based spectrum sensing scheme using a multi-antenna receiver. Our main idea is constructing a correlation matrix composed of not only auto-correlation functions per each antenna but also cross-correlation functions between antennas. By using the rich informative matrix, with a simple convolutional neural network (CNN) structure, our model, DS2MA (Deep Spectrum Sensing with Multiple Antennas), can efficiently learn to detect the presence of a primary user (PU). In our extensive simulation results, DS2MA using only auto-correlation functions for each antenna can outperform previous related works. By adding cross-correlation functions together, DS2MA can significantly improve the detection performance. We also show the impact of impulsive noise and correlation coefficient. The simulation results show that the proposed DS2MA provides a higher detection probability compared to the existing works regardless of the impulsive noise impact and correlation coefficient.**

***Index Terms*—Spectrum sensing, deep learning, auto-correlation, cross-correlation, single input multiple output (SIMO).**

I. Introduction

As RAPIDLY increasing the number of wireless communication devices and data rates, the scarcity of the spectrum band has become an important issue [1]. It has been reported that the current spectrum utilization policy shows a poor efficiency of spectrum usage due to spectrum bands remaining in an idle state, i.e., when licensed users do not occupy them [2]. To overcome the spectrum scarcity problem, cognitive radio (CR) has attracted considerable attention as a powerful candidate for improving the efficiency of spectrum usage [3], [4].

In CR systems, unlicensed users, i.e., secondary users (SUs), are allowed to occupy the spectrum bands if licensed primary users (PUs) do not occupy the spectrum bands [5]. Spectrum-sensing which detects the presence of a PU in the spectrum band is a key technique in CR systems [6]. In recent decades, spectrum-sensing schemes have been developed through mathematical rule-based approaches using signal energy [7], eigenvalue [8], and cyclostationary features [9], among others. In [10], a test statistic obtained by the weighted sum of the auto-correlated received samples is proposed. Single-input multiple-output (SIMO) receivers, which have multiple receiving antennas are widely used in wireless communication devices to obtain a lower error in noisy channels than those of the traditional receivers with single receiving antenna [11]. For multi-antenna receivers, the covariance matrix showing the statistical relationship between the received samples collected via different antennas has been adopted for spectrum sensing [12]. The spectrum-sensing schemes mentioned above have shown performance improvements in previous decades; however, such improvements can be severely degraded if the statistical channel model, which is assumed for spectrum sensing, does not match the real environment.

Recent studies have shown that deep learning can be effective in solving complicated problems. References [13] and [14] have adopted the covariance matrix as model input to a convolutional neural network (CNN) and a long short term memory (LSTM) model, respectively. References [15] and [16] adopted covariance matrices and PU activity pattern matrices simultaneously; however, they require a significant amount of information for generating activity pattern matrices. References [17] and [18] showed that auto-correlation operation-aided deep learning models can be effective for single-antenna CR devices. For modulation classification, [17] adopted auto-correlation to extract the periodicity of feature maps. In [18], the authors found that auto-correlation is an effective preprocessing for spectrum sensing.

This letter proposes a novel spectrum sensing scheme called deep spectrum sensing with multiple antennas (DS2MA) for multi-antenna receivers. We first show that the correlation matrices of received signals provide unique patterns which vary depending on whether the PU is present. We then design a novel CNN-based spectrum sensing model using correlation matrices as input. In the proposed scheme, we consider two types of correlation matrices. The first type is a matrix composed of auto-correlation functions for each antenna, which can be considered as an extension of the approach described in [18] to a multi-antenna receiver. For the second type, we focus on that cross-correlation functions are able to provide rich information on PU existence owing to their unique patterns. Accordingly, we propose to adopt a matrix constructed by concatenating the auto-correlation matrix and the cross-correlation matrix of the received samples collected through

Manuscript received 29 December 2022; revised 10 February 2023; accepted 19 February 2023. Date of publication 28 February 2023; date of current version 9 June 2023. This work was supported by the Institute of Information and Communications Technology Planning and Evaluation (IITP) Grant funded by the Korea Government (MSIT) through the Development of Incumbent Radio Stations Protection and Frequency Sharing Technology through Spectrum Challenge under Grant 2019-0-00964, through the Development of 5G Edge Security Technology for Ensuring 5G+ Service Stability and Availability under Grant 2020-0-00952, and through the AI Graduate School Support Program (Sungkyunkwan University) under Grant 2019-0-00421. The associate editor coordinating the review of this article and approving it for publication was C. Pan. *(Corresponding author: Yusung Kim.)*

Keunhong Chae is with the Department of Electrical and Computer Engineering, Sungkyunkwan University, Suwon 03063, Republic of Korea (e-mail: chae0820@skku.edu).

Yusung Kim is with the College of Computing and Informatics, Sungkyunkwan University, Suwon 03063, Republic of Korea (e-mail: yskim525@skku.edu).

Digital Object Identifier 10.1109/LWC.2023.3250257

different antennas. The proposed matrix shows the correlation between each antenna pair by patterns composed of multiple values, whereas the covariance matrices represent the correlation between each antenna pair with a single value. Owing to the rich information of the correlation matrices and a CNN model design suitable for correlation pattern classification, the proposed DS2MA model provides a better spectrum sensing performance than those of the existing deep learning models. Furthermore, we show that the DS2MA model which learns the auto-correlation and cross-correlation features simultaneously achieves a significant performance improvement compared with that of the DS2MA model trained using only auto-correlation matrices.

The main contributions of this letter can be summarized as follows: (i) This letter proposes adopting auto-correlation and cross-correlation functions simultaneously in spectrum sensing for multi-antenna receivers. (ii) The proposed model does not require complicated information such as previous activity pattern. (iii) Extensive simulation results show that the proposed model achieves a performance improvement of more than 4dB and 7dB over [13] and [15], respectively. Moreover, the proposed DS2MA shows a better performance compared to the conventional models even under non-Gaussian noise environment.

II. Signal Model

A. Spectrum Sensing

In CR systems, spectrum sensing can be modeled as a binary hypothesis testing problem, i.e.,

$$H_0 : y_i[n] = w_i[n], \tag{1}$$

and

$$H_1 : y_i[n] = x_i[n] + w_i[n], \tag{2}$$

where H_0 is a null hypothesis and H_1 is an alternative hypothesis, indicating that the PU is absent or present, respectively.

In addition, $x_i[n]$, $w_i[n]$, and $y_i[n]$ are the nth PU signal samples, noise samples, and received samples collected by the ith antenna, respectively. Here, $n = 0, 1, 2, \ldots, N-1$ and $i = 0, 1, 2, \ldots, M-1$, where N is the length of the received samples and M is the number of antennas.

B. Auto-Correlation

The auto-correlation function of $x_i[n]$ is expressed as

$$\Lambda_i^x(\tau) = \frac{1}{N}\sum_{n=0}^{N-1} x_i[n]x_i^*[n-\tau], \tag{3}$$

where $\tau = 0, 1, 2, \ldots, L-1$, $x_i[n] = x_i[n+N]$, $x_i^*[n]$ is the conjugate of $x_i[n]$, and L is the symbol duration. If the symbols are random, the correlation pattern of $\Lambda_i^x[\tau]$ is simply expressed as

$$\Lambda_i^x[\tau] = \begin{cases} 1 - \frac{|\tau|}{L}, & H_1 \\ 0, & H_0. \end{cases} \tag{4}$$

Fig. 1 shows the normalized auto-correlation functions of H_1 and H_0. $\Lambda_i^x[\tau]$ of H_1 gradually decreases as the delay

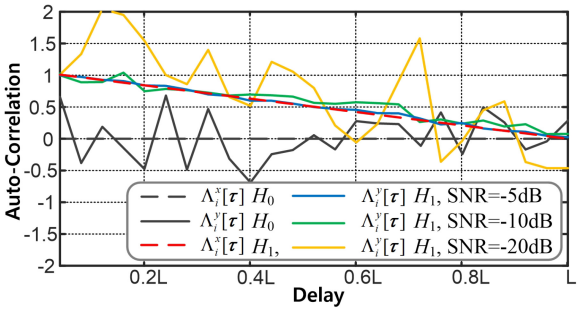

Fig. 1. The auto-correlation curves of H_0 and H_1.

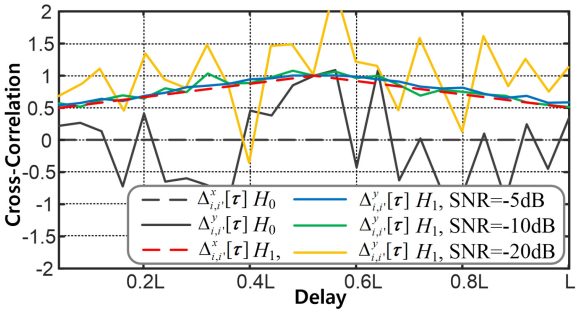

Fig. 2. The cross-correlation curves of H_0 and H_1 obtained by two adjacent antennas.

increases according to Equation (4), and thus, is able to differentiate clearly from that of H_0. Even though the correlation patterns $\Lambda_i^y[\tau]$, i.e., the correlation function including correlated noise are degraded compared to those of $\Lambda_i^x[\tau]$, decreasing pattern can be still observed visually at the very low signal-to-noise ratio (SNR).

In the proposed model, we adopt the auto-correlation function matrix of signal $y_i[n]$ which can be expressed as

$$\phi_{i,\tau} = \frac{1}{N}\sum_{n=0}^{N-1} y_i[n]y_i^*[n-\tau], \tag{5}$$

where $\phi_{i,\tau}$ is the element of the auto-correlation matrix Φ.

C. Cross-Correlation

The cross-correlation function matrix of signal $x_i[n]$ and $x_{i'}[n]$ can be expressed as

$$\Delta_{i,i'}^x(\tau) = \frac{1}{N}\sum_{n=0}^{N-1} x_i[n]x_{i'}^*[n-\tau], \tag{6}$$

where $i' = 0, 1, 2, \ldots, M-1$ and $i \neq i'$. Fig. 2 shows the normalized cross-correlation functions of H_1 and H_0 obtained by two closest antennas, where the correlation coefficient [15] ρ is set to 0.5. Due to delay between antennas, the shape of the cross-correlation obtained by two adjacent antennas is same with that of $\Lambda_i^x[\tau - L\rho]$ as depicted in Fig. 2. Similar to those of the auto-correlation, the delayed correlation pattern is able to observed visually at the very low SNR. Thus, it is expected that the classification accuracy can be further improved if the cross-correlations are additionally adopted for spectrum sensing.

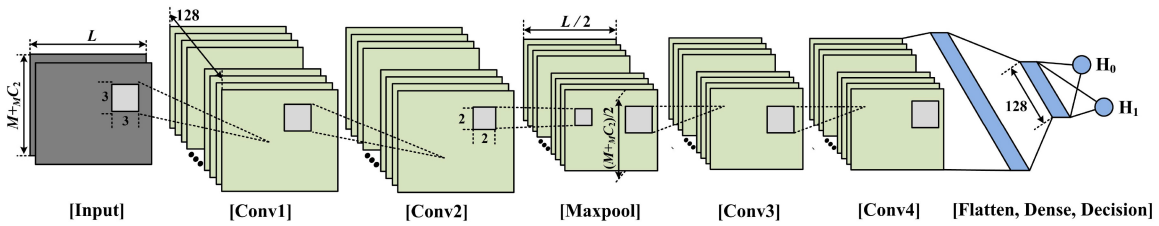

Fig. 3. The model design of the proposed DS2MA model.

In the proposed model, we adopt the cross-correlation function matrix of signal $y_i[n]$ and $y_{i'}[n]$ which can be expressed as

$$\psi_{c,\tau} = \frac{1}{N}\sum_{n=0}^{N-1} y_i[n] y_{i'}^*[n-\tau], \tag{7}$$

where $\psi_{c,\tau}$ is the element of the cross-correlation matrix Ψ, and c is an index representing different cross-correlations and thus satisfies $c = 0, 1, 2, \ldots, {}_M C_2$.

III. DS2MA Model

To embed the data, we propose two types of correlation matrices. The first type is the auto-correlation matrix which can be considered as an extension of [18]. The embedded data are shaped to contain real and imaginary components of Φ for the first and second channels, respectively. Thus, the size of the embedded data is equal to $M \times L \times 2$. In addition, we propose a concatenation of the cross-correlation matrices to the auto-correlation matrices. Similar to auto-correlation matrices, the embedded data are shaped to contain real and imaginary components on each channel, and thus, the size of the embedded data is equal to $(M +_M C_2) \times L \times 2$.

Because the DS2MA model is trained to classify whether a PU is present, the DS2MA model is trained through supervised learning with binary labels. The labeled dataset can be expressed as (Φ_k, l_k), where Φ_k and l_k are the kth auto-correlation matrix and the corresponding binary-digit label, respectively. Fig. 3 shows the design of the proposed DS2MA model. The proposed model is composed of four convolution layers, one max pool layer between two convolution layers, and dense layers with a softmax activation layer at the end of the model. A kernel size of 3×3 is adopted for each CNN layer, and the width and height of the data are kept constant by using zero-padding and the kernel stride length of 1, except for the maxpool layer, thereby reducing the width and height of the data by half. After flattening the hidden layers, the activation layer estimates the score representing the probability of the PU status, $[P_{H_0}(\Phi_k|\theta), P_{H_1}(\Phi_k|\theta)]$ where $P_{H_0}(\Phi_k|\theta)$ and $P_{H_1}(\Phi_k|\theta)$ represent the estimated probability score of whether the PU is absent or present, respectively, and θ is the model parameter after training. Table I lists the specific model structures.

During the training sequence, the cross-entropy function is adopted as a loss function, which can be expressed as

$$L(\theta) = -\sum_{k=1}^{K} l_k \log(P_{H_1}(\Phi_k|\theta)) + (1 - l_k)\log(P_{H_0}(\Phi_k|\theta)). \tag{8}$$

TABLE I
DS2MA Model Structure

Input Size: $(M+_MC_2) \times L \times 2$		
Layers	**Kernel Size (CNN/Maxpool) Number of Nodes (Dense)**	**Activation Function**
Input Layer	N/A	N/A
Conv 1	(3 × 3) @ 128	ReLu
Conv 2	(3 × 3) @ 128	ReLu
Maxpool	(2 × 2) @ 128	N/A
Conv 3	(3 × 3) @ 128	ReLu
Conv 4	(3 × 3) @ 128	ReLu
Flatten	N/A	N/A
Dense	128	ReLu
Decision	2	Softmax
Output Size: 2 × 1		

Here, the stochastic gradient descent (SGD) optimizer is selected for reducing the loss function. Except for the last activation layer, the activation function of the other layers is set as ReLU. The learning rate of 0.0005 is selected for this letter, and the number of training epochs is set to 50 with the early-stopping patience of 10.

IV. Simulation Results

For simulation, we generated quadrature phase-shift keying (QPSK) samples under independent and identically distributed (i.i.d.) complex Gaussian noise channel. The parameters are set as follows: $N = 1{,}000$, $L = 25$, and $M = 8$. The numbers of data for training and testing are 30,000 and 15,000 for each SNR, respectively, where 20% of the training dataset is randomly used as the validation set. To prevent overfitting, we generated the training and test datasets independently and monitored validation losses for every epoch. The SNR range of −25 to −17 dB with 1-dB intervals is considered. Here, the SNR of the training data is assumed to follow uniform distribution within the interval of ±1 dB from the target SNR to consider noise uncertainty. The proposed DS2MA model is divided into two types: 'DS2MA (A only)' utilizing only auto-correlation (Φ) and 'DS2MA (A+C)' utilizing auto-correlation (Φ) and cross-correlation (Ψ) simultaneously. We compare DS2MA, energy detection (ED) [7], and deep covariance matrix CNN (CM-CNN) [13] in terms of detection probability defined as $P_d = Pr(H_1|H_1)$. Although activity pattern aware spectrum sensing (APASS) [15] requires approximately 16 times more samples than DS2MA, CM-CNN, and ED due to the activity pattern matrices, APASS is also included in the simulation results. The parameters of CM-CNN and APASS are set to follow the descriptions presented in existing works. The generated dataset is uploaded on IEEE Dataport [19].

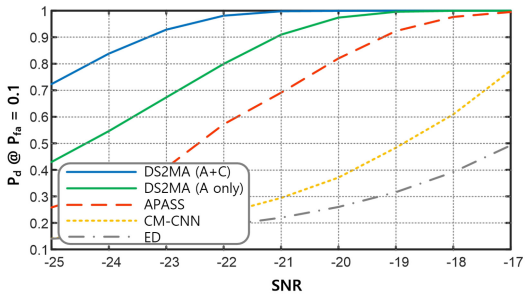

Fig. 4. P_d of the proposed and conventional schemes as a function of SNR when $\rho = 0.5$.

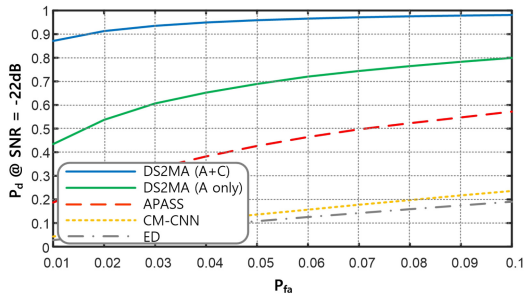

Fig. 5. ROC curves of the proposed and conventional schemes when $\rho = 0.5$.

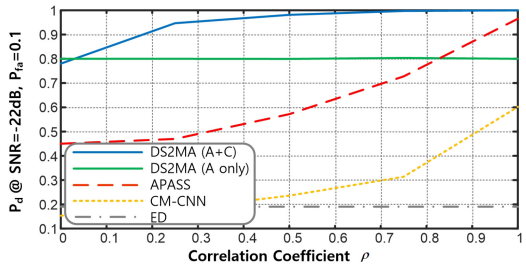

Fig. 6. P_d of the proposed and conventional schemes as a function of ρ.

Fig. 4 compares the detection probability of the proposed DS2MA model with conventional schemes, where the false alarm probability, defined as $P_{fa} = Pr(H_1|H_0)$ is set to 0.1 and $\rho = 0.5$. The figure clearly confirms that the proposed DS2MA exhibits a higher detection probability than conventional spectrum sensing schemes. In addition, the DS2MA (A+C) model shows a significantly improved detection performance compared to the DS2MA (A only) model. It can be interpreted that the additional correlation statistics obtained via cross-correlations affect the probability of successful PU detection. Fig. 5 shows the receiver operating characteristic (ROC) curves of the proposed and conventional spectrum-sensing schemes, where SNR $= -22$ dB. The figure clearly shows that the proposed DS2MA (A+C) model exhibits an improved detection probability over conventional schemes of at least 0.4, and shows a higher area under the ROC curve (AUC) of 0.9532 than those of [15] (0.4198) and [13] (0.1441).

Because the correlation coefficient ρ may vary depending on the antenna arrangement or the reception angle, it is impractical to guarantee that ρ is fixed at a single value. Fig. 6 shows

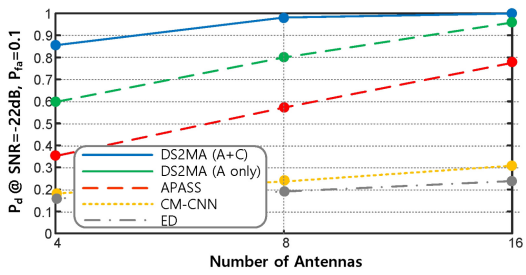

Fig. 7. P_d of the proposed and conventional schemes as a function of M when $\rho = 0.5$.

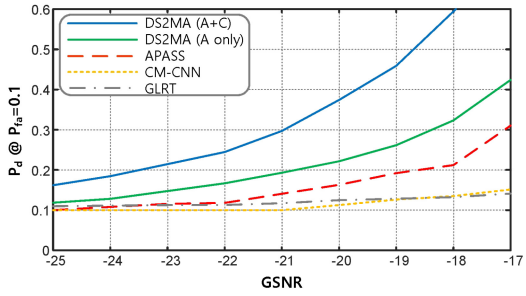

Fig. 8. P_d of the proposed and conventional schemes as a function of generalized SNR (GSNR) under Cauchy noise when $\rho = 0.5$.

the detection probability performance of the proposed and conventional spectrum-sensing schemes as a function of ρ where the SNR $= -22$ dB and $P_{fa} = 0.1$. As shown in the figure, the detection probability of DS2MA (A+C) gradually increases as ρ increases as expected. APASS and CM-CNN also show increasing detection probabilities as ρ increases, but they show lower detection probabilities than those of DS2MA (A+C) regardless of the value of ρ. Since the auto-correlation matrix does not affected by ρ, DS2MA (A only) shows detection probabilities independent to ρ.

Fig. 7 shows the detection probability of the proposed and conventional spectrum sensing schemes as a function of M, where $M = 4$, 8, and 16 are additionally considered. The samples per antenna $N = 1{,}000$ is considered as the simulations above. From Fig. 7, it is confirmed that the detection performance of the spectrum sensing schemes of interest increases as the number of antennas increases as expected, and the proposed DS2MA (A+C) shows the best detection performance compared with the conventional schemes regardless of the number of antennas.

To evaluate DS2MA under complicated noise scenarios, the detection performances are compared under non-Gaussian impulsive noise environments modeled by Cauchy distribution [20]. In simulation, ED is replaced to generalized likelihood ratio test (GLRT) which is widely used under non-Gaussian noise environments. In order to exclude highly impulsive noise samples, the received samples higher than 3γ and lower than -3γ were replaced to 3γ and -3γ, respectively, where γ is the dispersion of the Cauchy noise. As depicted in Fig. 8, it can be seen that all schemes suffer performance degradation under Cauchy noise, but DS2MA still achieve the highest probability of detection.

TABLE II
COMPLEXITY COMPARISON

Model	# of Model Parameters	Average Time for detection	Required Memory (Compressed Model)
DS2MA (A+C)	3,984,514	34.19ms	15.59MB (3.91MB)
DS2MA (A Only)	1,232,002	33.77ms	4.84MB (1.22MB)
APASS	8,538,162	37.17ms	33.90MB
CM-CNN	76,210	31.95ms	0.33MB

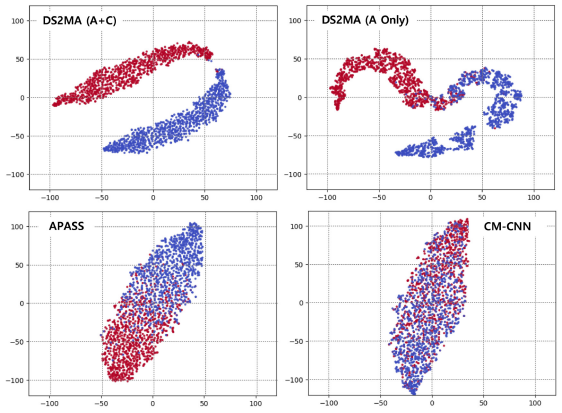

Fig. 9. t-SNE results when SNR=−20dB.

Table II compares the complexity of the proposed and existing spectrum sensing models in terms of the number of model parameters, average time for detection, and required memory. Here, all spectrum sensing schemes of interest are tested by using Intel Xeon 5220R 24C/48T processor. The table shows that the proposed DS2MA achieves a lower complexity compared to APASS. Moreover, it is shown that the memory usage could be further reduced by adopting the compressed models with the detection probability degradation of 0.042% on average.

Fig. 9 shows t-distributed stochastic neighbor embedding (t-SNE) figures of the proposed and conventional spectrum sensing models when SNR = −20 dB, where red and blue dots denote the PU is present and absent, respectively. From the figure, it is clearly seen that the labels of the DS2MA (A+C) are clustered better than those of other schemes. DS2MA (A only) also shows a better classification performance compared to APASS and CM-CNN. In contrast, on t-SNE figures of APASS and CM-CNN, they are frequently observed that different labels exist on similar locations.

V. CONCLUSION

In this letter, we have proposed a spectrum sensing model for multi-antenna receivers. We have obtained auto-correlation and cross-correlation matrices from the samples collected by multiple antennas. Using the matrices as input, we have designed a CNN-based spectrum sensing model. Our extensive simulation results have confirmed that the proposed model achieves a better detection performance than the related studies. In addition, our model shows the best performance advantage under the impulsive noise channel. For future research, the authors consider analyzing the influence of correlated noise caused by correlation operation and developing deep learning models adopting advanced learning methods such as self-supervised learning, etc.

REFERENCES

[1] S. Haykin, D. J. Thomson, and J. H. Reed, "Spectrum sensing for cognitive radio," *Proc. IEEE*, vol. 97, no. 5, pp. 849–877, May 2009, doi: 10.1109/JPROC.2009.2015711.
[2] "Notice of proposed rule making and order: Facilitating opportunities for flexible, efficient, and reliable spectrum use employing cognitive radio technologies," Federal Commun. Commission, Washington, DC, USA, Rep. 03–108, 2003.
[3] J. Mitola, "Cognitive radio: An integrated agent architecture for software defined radio," Ph.D. dissertation, Dept. Teleinformatics, Roy. Inst. Technol. (KTH), Stockholm, Sweden, 2000.
[4] A. Ali and W. Hamouda, "Advances on spectrum sensing for cognitive radio networks: Theory and applications," *IEEE Commun. Surveys Tuts.*, vol. 19, no. 2, pp. 1277–1304, 2nd Quart., 2017, doi: 10.1109/COMST.2016.2631080.
[5] S. Haykin, "Cognitive radio: Brain-empowered wireless communications," *IEEE J. Sel. Areas Commun.*, vol. 23, no. 2, pp. 201–220, Feb. 2005, doi: 10.1109/JSAC.2004.839380.
[6] E. Axell, G. Leus, E. G. Larsson, and H. V. Poor, "Spectrum sensing for cognitive radio: State-of-the-art and recent advances," *IEEE Signal Process. Mag.*, vol. 29, no. 3, pp. 101–116, May 2012, doi: 10.1109/MSP.2012.2183771.
[7] F. F. Dighan, M.-S. Alouini, and M. K. Simon, "On the energy detection of unknown signals over fading channels," in *Proc. Int. Conf. Commun. (ICC)*, 2003, pp. 3575–3579, doi: 10.1109/ICC.2003.1204119.
[8] Y. Zeng, C. L. Koh, and Y.-C. Liang, "Maximum eigenvalue detection: Theory and application," in *Proc. IEEE Int. Conf. Commun.*, 2008, pp. 4160–4164, doi: 10.1109/ICC.2008.781.
[9] F. Salahdine, H. El Ghazi, N. Kaabouch, and W. F. Fihri, "Matched filter detection with dynamic threshold for cognitive radio networks," in *Proc. Int. Conf. Wireless Netw. Mobile Commun. (WINCOM)*, 2015, pp. 1–6, doi: 10.1109/WINCOM.2015.7381345.
[10] T. Ikuma and M. Naraghi-Pour, "Autocorrelation-based spectrum sensing algorithms for cognitive radios," in *Proc. 17th Int. Conf. Comput. Commun. Netw.*, 2008, pp. 1–6, doi: 10.1109/ICCCN.2008.ECP.102.
[11] R. Ayoubi and J. Daba, "FPGA design of spatially modulated single-input-multiple-output signals in 5G diversity receivers," in *Proc. IEEE Int. Conf. Commun. Netw. Satell. (Comnetsat)*, 2019, pp. 24–29, doi: 10.1109/COMNETSAT.2019.8844099.
[12] Y. Zeng and Y.-C. Liang, "Spectrum-sensing algorithms for cognitive radio based on statistical covariances," *IEEE Trans. Veh. Technol.*, vol. 58, no. 4, pp. 1804–1815, May 2009, doi: 10.1109/TVT.2008.2005267.
[13] X. Liu, J. Wang, X. Liu, and Y.-C. Liang, "Deep CM-CNN for spectrum sensing in cognitive radio," *IEEE J. Sel. Areas Commun.*, vol. 37, no. 10, pp. 2306–2321, Oct. 2019, doi: 10.1109/JSAC.2019.2933892.
[14] W. Chen, H. Wu, and S. Ren, "CM-LSTM based spectrum sensing," *Sensors*, vol. 22, no. 6, p. 2286, 2022, doi: 10.3390/s22062286.
[15] J. Xie, X. Liu, Y.-C. Liang, and J. Fang, "Activity pattern aware spectrum sensing: A CNN-based deep learning approach," *IEEE Commun. Lett.*, vol. 23, no. 6, pp. 1025–1028, Jun. 2019, doi: 10.1109/LCOMM.2019.2910176.
[16] J. Xie, J. Fang, C. Liu, and X. Li, "Deep learning-based spectrum sensing in cognitive radio: A CNN-LSTM approach," *IEEE Commun. Lett.*, vol. 24, no. 10, pp. 2196–2200, Oct. 2020, doi: 10.1109/LCOMM.2020.3002073.
[17] D. Zhang, W. Ding, C. Liu, H. Wang, and B. Zhang, "Modulated autocorrelation convolution networks for automatic modulation classification based on small sample set," *IEEE Access*, vol. 8, pp. 27097–27105, 2020, doi: 10.1109/ACCESS.2020.2971586.
[18] K. Chae, J. Park, and Y. Kim, "Rethinking autocorrelation for deep spectrum sensing in cognitive radio networks," *IEEE Internet Things J.*, vol. 10, no. 1, pp. 31–41, Jan. 2023, doi: 10.1109/JIOT.2022.3200968.
[19] K. Chae, 2022, "Simulation training/test data for DS2MA spectrum sensing model: Baseband QPSK," IEEE DataPort, doi: 10.21227/qs1q-wc83.
[20] S. Gurugopinath, R. Muralishankar, and H. N. Shankar, "Spectrum sensing in the presence of cauchy noise through differential entropy," in *Proc. IEEE Distrib. Comput. VLSI Electr. Circuits Robot.*, 2016, pp. 201–204, doi: 10.1109/DISCOVER.2016.7806266.